



Parameter Optimization Analysis of The New Straw Brick Based on Thermal Performance

Wanjun Hou^{1,2}, Shi Zhao^{1,2}, Juanli Guo^{1,3,*}, Hui Xi^{1,2}, Ziyu Chen^{1,2}, Renjie Xu⁴

¹ School of Architecture, Tianjin University, Tianjin, 300072, China

² School of Architecture and Art, Hebei University of Engineering, Handan, 056000, China

³ Tianjin Key Laboratory of Architectural Physics and Environmental Technology, Tianjin University, Tianjin, 300072, China

⁴ Tianjin International Engineering Institute, Tianjin University, Tianjin 300072, China

*Email address: guojuanli@tju.edu.cn

Abstract. In this study, the thermal properties of the new straw bricks produced at high temperatures and pressure were explored and the pattern of influence of pore diameter on the heat transfer coefficient of the new straw bricks was emphasized. The thermal environment of the experimental house with new straw bricks was monitored and then the building model and the numerical model of the new straw bricks were built in DesignBuilder and COMSOL Multi-physics software, respectively. The influence of the hole diameter on the thermal performance of the new straw bricks was analyzed to obtain the design parameters when the thermal performance of the new straw bricks was optimal. The optimum value for hole diameter is 30 mm when the new straw bricks of 150 mm have the lowest heat transfer coefficient.

Keywords: New straw brick; Thermal performance; Heat transfer coefficient

1 Introduction

China has abundant straw resources, and straw bricks have the advantages of heat insulation, reducing building energy consumption, etc. [1,2]. Using straw bricks as building wall materials can significantly reduce construction costs, and achieve sustainable use of resources [3].

The performance of straw bricks produced by the baling method is a major concern of current research. Jin et al. [4] concluded that the heat transfer coefficient of straw brick walls is significantly lower than that of sintered clay brick walls. And the indoor thermal comfort of straw brick houses was significantly enhanced. Research and practice of bale straw bricks have been carried out in countries such as the USA, Canada, Australia, and the UK [5,6]. However, Collet et al. [7] pointed out that the production of straw bales requires a high level of equipment. Manual handling leads to changes in the density of the straw bales, which weakens their thermal properties.

Focused on these problems, a new straw brick produced by high temperature and pressure is proposed in this study. The density of the new straw brick is 300–600 kg/m³

© The Author(s) 2023

D. Li et al. (eds.), *Proceedings of the 2023 9th International Conference on Architectural, Civil and Hydraulic Engineering (ICACHE 2023)*, Advances in Engineering Research 228,

https://doi.org/10.2991/978-94-6463-336-8_4

and its thermal conductivity was experimentally measured to be $0.13 \text{ W}/(\text{m}\cdot\text{K})$. The mechanized production reduces the effect of manual handling on the thermal performance of the new straw brick, but the heating rods responsible for the high-temperature effect leave three holes of the same diameter inside the new straw brick. Therefore, this study focused on the effect of the diameter of the holes on the heat transfer coefficient of the new straw bricks and explored the parameters of the new straw bricks with optimum thermal performance. In addition, the economic and thermal properties of the new straw bricks were taken into account to explore the parameters of the new straw bricks when the total investment is minimal and to suggest parameters for new straw bricks that are suitable for wider application.

2 Materials and methods

2.1 Properties and production process of new straw bricks

New straw bricks are produced under high temperatures and pressure. Straw and environmentally friendly binders are the main raw materials for new straw bricks.

The process of producing new straw bricks consists of six steps. The first step is to collect the straw from the fields and bale it for storage. The second step is to crush the straw in a shredder. Finely crushed straw can have a good binding effect and enhance the hardness of the new straw bricks. If the particles are too large in diameter, the new straw bricks may swell and the yield of the new straw bricks is reduced. In the third step, the crushed straw is put into a dryer for drying. In the fourth step, the dried straw mash and the organic binder are put into the production equipment and mixed evenly. The use of an organic binder reduces the weight of the new straw bricks compared to the inorganic binder. In the fifth step, the straw mash is heated using three heating rods evenly spaced in the production equipment. The high temperature speeds up the bonding of the binder to the straw mash. At the same time, high pressure is applied to the material to increase the density of the new straw bricks. The sixth step is to adjust the length of the grass tiles in the appropriate mold by cutting them. Photographs of the production process are shown in Figure 1.



(a)



(b)



(c)



Fig. 1. New straw bricks production process.

2.2 Experimental house

A single-story building with new straw bricks as walls has been built on the south side of the Water Conservancy Hall on the Weijin Road campus of Tianjin University. In this study, the building was chosen to test the thermal performance of the new straw bricks. The experimental house area is 23.86 m², with a size of 4.4 m × 5.0 m. The building height is 3.7 m and the window-to-wall ratio is 0.19 for south-facing windows and 0.15 for east-facing windows.

The natural indoor temperature of the experimental house was measured with the Onset HOBO temperature and humidity recorders. The technical specifications of the test instrument are shown in Table 1. To meet the requirement of indoor and outdoor temperature difference of more than 10° during the test period, a six-day indoor and outdoor air temperature test was conducted between the Winter Solstice and the Minor Cold (from December 26th to December 31st, 2021). The test periods were all under sunny working conditions. The thermal performance of the wall can be measured by testing the air temperature obtained from a building without any active heating and cooling measures. Consequently, no heating equipment was operated inside the experimental house during the test period.

Table 1. Technical parameters of the test instrument

Instrument	Parameters	Range	Error
Onset HOBO temperature and humidity	<i>t</i>	-20–70 °C	±0.21 °C

It's worth noting that the data recording interval was set to 30 minutes according to the building's average indoor temperature detection method. The instrument was placed at a height of 1.5 m above the floor and also 1 m from the internal surfaces of the walls on both sides. The building plan and the location of the measurement points are shown in Figure 2.

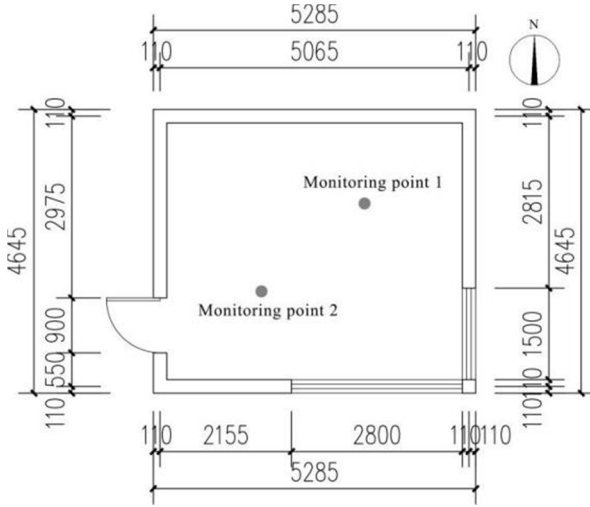


Fig. 2. Plan of the new straw brick building and marking of the location of the survey points.

When the room is larger than 16 square meters, two instruments need to be placed equally on the diagonal of the experimental house. The data obtained from the experiment requires a further calculation of the natural room temperature using Equations (1) and (2) [8].

$$t_{rm} = \frac{\sum_{i=1}^n t_{rm,i}}{n} \quad (1)$$

$$t_{rm,i} = \frac{\sum_{j=1}^p t_{i,j}}{p} \quad (2)$$

where t_{rm} is the average of the natural room temperature of the building, °C; $t_{rm,i}$ is the i -th hourly natural room temperature value, °C; n is the number of hourly natural room temperature data obtained by monitoring; $t_{i,j}$ is the hour-by-hour value of the i th natural room temperature at the j -th measurement point; p is the number of measurement points in the building interior.

2.3 Basic model

The thermal performance of a wall can be measured by the heat transfer coefficient [9]. Enhancement of thermal performance can decrease the building's energy consumption and cut building energy costs.

The heat transferred per unit of time through 1 square meter of the wall is the heat transfer coefficient, when the difference in air temperature between the two sides of the wall is 1 °C (1 °C=274.15 K). For example, if the new straw bricks are treated as a homogeneous wall, the heat transfer coefficient can be calculated using Equation (3) [10].

$$K = \frac{1}{\frac{1}{\alpha_n} + \frac{\delta}{\lambda} + \frac{1}{\alpha_w}} \quad (3)$$

where K is the heat transfer coefficient of the new straw brick wall, $W/(m^2 \cdot K)$; α_n is the heat transfer coefficient of the inner surface of the new straw brick wall, which is taken to be $8.7 W/(m^2 \cdot K)$; α_w is the external surface heat transfer coefficient of the new straw brick wall, which is taken to be $23 W/(m^2 \cdot K)$; δ is the thickness of the new straw bricks, m; λ is the thermal conductivity of the new straw bricks, $W/(m^2 \cdot K)$. According to the experimental data from the research team's completed study, the thermal conductivity of the new straw bricks was taken to be $0.13 W/(m^2 \cdot K)$.

To determine whether the heat transfer coefficient of the new straw bricks calculated by Equation (3) is reasonable, DesignBuilder was used in this study to numerically simulate the thermal performance of the experimental house. Figures 3 and 4 show the actual photograph of the experimental house and the numerical simulation model respectively. The heat transfer coefficients of the new straw bricks calculated by Equation (3) were entered into the DesignBuilder and Table 2 shows the other main parameters used in the simulation. Tianjin's meteorological conditions are the basis for the simulations and the experimental house is located here.



Fig. 3. Photograph of the experimental house.

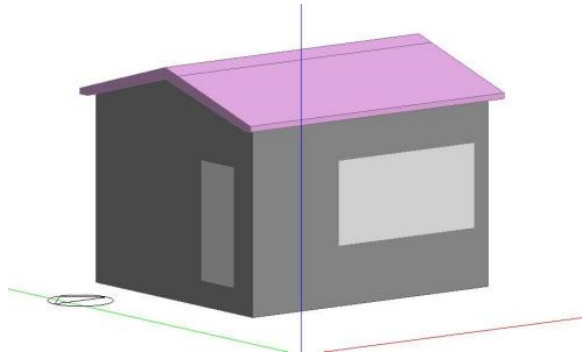


Fig. 4. Numerical simulation model.

Table 2. Parameters for numerical simulation

	New straw brick wall	Pitched roof	Interior floor	Window	Door
Thermal resistance [[K·m ²)/W]	7.874	1.748	0.224	0.17	0.351

3 Results and discussion

3.1 Monitoring data analysis

Figure 5 shows the monitoring results of the indoor and outdoor temperatures from 26 to 31 December. While the average outdoor temperature increased by 6.0 °C, the average indoor temperature only increased by 2.8 °C. The average indoor temperature fluctuation was smaller than the average outdoor temperature fluctuation. The monitoring results indicate that the new straw brick wall is beneficial in maintaining a stable indoor temperature. In addition, the maximum difference between indoor and outdoor temperatures was 4.7 °C, indicating that the new straw brick wall used in this experimental room has good thermal performance and contributes to the comfort of the indoor environment.

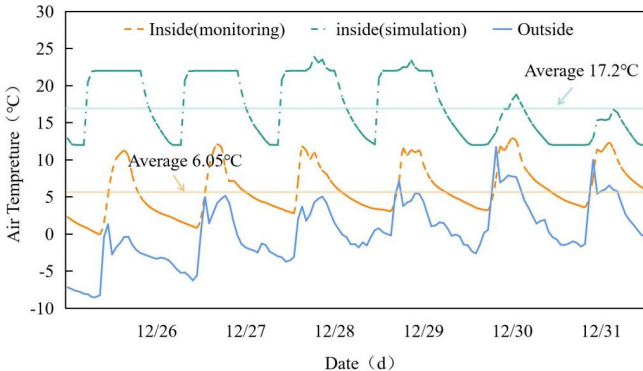


Fig. 5. Simulation and monitoring results of air temperature.

The results of the numerical simulation of the inside temperature in the experimental house are also presented in Figure 5. The comparison study found that the simulated inside temperature fluctuation trend was approximately the same as the monitored data. However, the simulated indoor temperature fluctuation of 11.88 °C was lower than the fluctuation of 12.92 °C from the monitoring data. The simulated mean indoor temperature of 17.2 °C was much higher than the mean of 6.05 °C from the monitoring data. This phenomenon indicated that there was a deviation between the theoretically calculated value of the heat transfer coefficient of the new straw bricks obtained by Equation (3) and the actual situation. Therefore, it was inappropriate to consider the

new straw brick walls as homogeneous walls and the influence of the holes inside the new straw bricks on the heat transfer coefficient cannot be ignored.

3.2 Numerical simulation

As a result of the production process, the heating rods responsible for the high temperature led to the creation of three circular holes in the new straw bricks, which has an impact on the thermal performance of the new straw bricks. The large deviations between the actual and theoretical values of the heat transfer coefficient of the new straw bricks were due to neglecting the holes.

To verify the above assumption, the simulation program of the effect of pore size was run on the thermal performance of the new straw bricks using COMSOL Multi-physics software. The software created a two-dimensional model of the cross-section of a new straw brick for the experimental house. The model's left side was set to outdoor conditions and the right side was set to indoor conditions. Winter meteorological data in Tianjin was chosen as the condition for the numerical simulation. The outdoor temperature in winter was $-10.57\text{ }^{\circ}\text{C}$ and the indoor temperature was taken as $18\text{ }^{\circ}\text{C}$. The heat exchange coefficient of the inner surface of the new straw bricks was taken as $8.7\text{ W}/(\text{m}^2\cdot\text{K})$ and the heat exchange coefficient of the outer surface was taken as $23\text{ W}/(\text{m}^2\cdot\text{K})$ [10]. Figures 6 and 7 show the two-dimensional model and the meshing of the cross-section of the new straw bricks respectively.

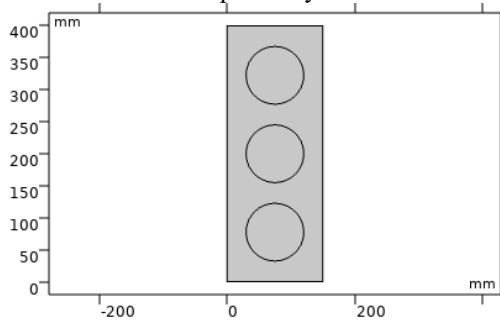


Fig. 6. Model of a cross-section of the new straw bricks.

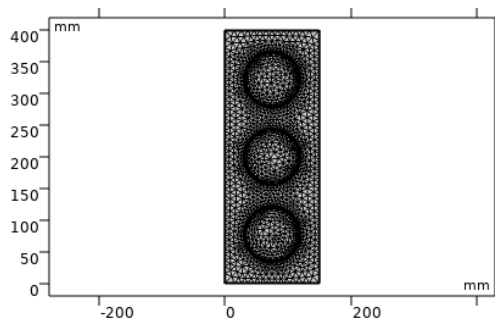


Fig. 7. The meshing of the model.

Model reliability validation.

Using the specifications of the new straw bricks used in the experimental room as a basis, the pore size of the new straw bricks model was set to 90 mm. The heat flow density was then calculated to be 24.62 W/m², which in turn led to a heat transfer coefficient of 0.862 W/(K·m²). This heat transfer coefficient was entered into the DesignBuilder to simulate the natural indoor temperature of the experimental house. The mean bias error (MBE) and the coefficient of variation of root mean square error (CV_{RMSE}) were calculated according to Equations (4) and (5) to determine the reliability of the model [11].

$$MBE = \frac{\sum(S-T)_{in}}{\sum T_{in}} \cdot 100\% \quad (4)$$

$$CV_{RMSE,p} = \frac{N \cdot \sqrt{\frac{\sum(S-T)_{in}^2}{N}}}{\sum T_{in}} \quad (5)$$

where S is the simulated value of natural indoor temperature, °C; N is the natural indoor temperature monitoring value, °C; T is the number of hours, h; in is the interval between the collection of natural room temperature data.

A comparison of monitoring and simulation results of air temperature is shown in Figure 8. The MBE was calculated to be 1.94% ($\leq 5\%$) and the CV_{RMSE} was 8.67% ($\leq 15\%$), both of which were reasonable. Therefore, the model was reliable.

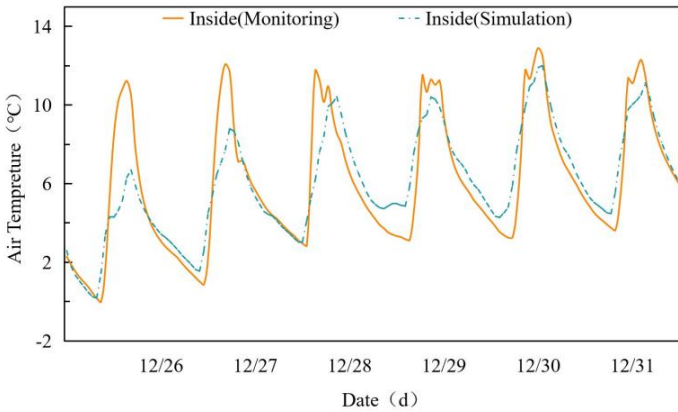


Fig. 8. Comparison of monitoring and simulation results of air temperature.

Parametric analysis of the pore size.

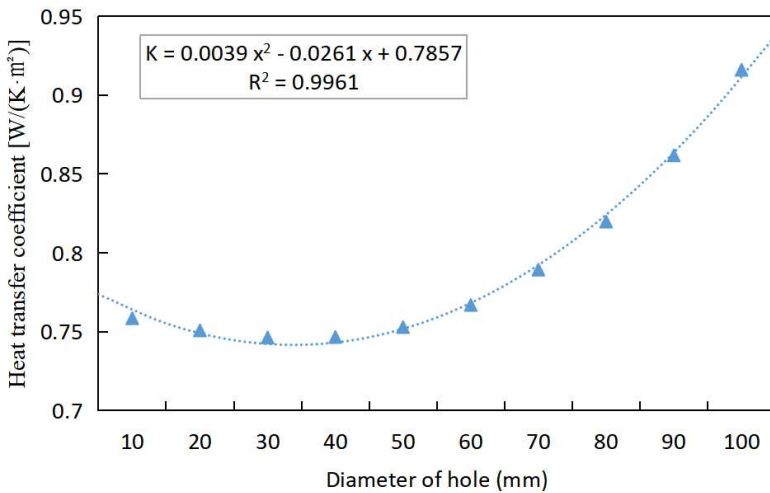
Using a new straw brick with a width of 150 mm as an example, simulations were carried out to calculate the effect of varying the hole diameter from 10 mm–100 mm on the thermal performance of a new straw brick. The simulation was set at 10 mm intervals. The results of the calculations are summarized in Table 3.

Table 3. Values of heat transfer coefficients corresponding to different hole diameters

Width of new straw bricks (mm)	Diameter of the hole (mm)	Heat flow density (W/m ²)	Heat transfer coefficient [W/(K·m ²)]	Energy consumption of buildings (kWh)
150	10	21.67	0.758	3230.780
	20	21.45	0.751	3219.533
	30	21.32	0.746	3212.707
	40	21.33	0.747	3213.552
	50	21.51	0.753	3223.018
	60	21.91	0.767	3243.983
	70	22.55	0.789	3277.493
	80	23.42	0.820	3322.595
	90	24.62	0.862	3384.545
	100	26.17	0.916	3460.980

Based on the data in Table 3, a regression analysis was conducted with the hole diameter as the independent variable and the straw brick's heat transfer coefficient as the dependent variable. Equation (6) is the regression equation.

$$K = 0.0039 \cdot x^2 - 0.0261 \cdot x + 0.7857 \quad (6)$$

**Fig. 9.** Regression curve of hole diameter and heat transfer coefficient.

The regression results for hole diameter and new straw bricks heat transfer coefficient are shown in Figure 9. The R-squared of the regression equation is 0.9961, indicating that 99.61% of the data can be explained by Equation (6). Therefore, the regression equation is reasonable.

The heat transfer coefficient of the new straw bricks shows a pattern of change with the increase of the diameter of the holes, which first decreases and then increases. When the diameter of a hole is greater than 30 mm, the thermal performance of the new

straw bricks is positively related to the hole diameter. The stronger airflow movement in the hole has a negative impact on the thermal performance of the new straw bricks. In summary, the 30 mm hole diameter is the optimum value for the new 150 mm new straw brick, where the heat transfer coefficient of $0.746 \text{ W}/(\text{K}\cdot\text{m}^2)$ is minimal and the energy-saving effect is the best. Compared to new straw bricks with a 90 mm hole diameter, the energy consumption of 171.838 kWh was reduced after applying new straw bricks with a 30 mm hole diameter.

4 Conclusions

Based on the monitoring of the thermal performance of the new straw brick application examples, it was found that the hole size influences the heat transfer coefficient of the new straw brick. The pattern of influence of hole diameter on the heat transfer coefficient of the new straw brick wall was analyzed, leading to the following conclusions:

The increase in the diameter of the holes leads to a change in the heat transfer coefficient of the new straw bricks, which first increases and then decreases. For straw bricks with a thickness of 150 mm, the heat transfer coefficient is minimal when the hole diameter is 30 mm. In addition, the greater the thickness of the new straw bricks is, the greater the diameter of the holes allowed at the lowest heat transfer coefficient will be.

References

1. Stone N. (2003) Thermal performance of straw bale wall systems. *Ecological Building Network*, 1-7. https://www.ecobuildnetwork.org/images/straw_bale_papers/Thermal_Performance_of_Straw_Bale_Wall_Systems_Stone_2003.pdf
2. Collet F, Serres L, Miriel J, Bart, M (2006) Study of thermal behavior of clay wall facing south. *Building & Environment*, **41** 307-315. <https://doi.org/10.1016/j.buildenv.2005.01.024>
3. Cai J Ling, Liu J, Wang N Ke, Zhang Y Qin, Wang J, (2021) Research progress on comprehensive utilization of crop straw. *Journal of Anhui Agricultural Sciences*, **49** 11-14. https://hfffgc1d129f57bb244a4snu9cknf6nk006o0ufgfy.eds.tju.edu.cn/kcms2/article/abstract?v=3uoqIhG8C44YLTIOAiTRKibY1V5Vjs7iy_Rpms2pqwbFRRUtoUImHZqkiQjI1Rp54IP5F8H2NRYQtEqESkzKa7ZSxVN5qUUX&uniplatform=NZKPT
4. Jin H, Shao T, Jin Y Meng, Kang J, (2016) The application of passive technology on rural houses in severe cold regions. *Journal of Human Settlements in West China*, **31** 115-118. <https://doi.org/10.13791/j.cnki.hsfwest.20160120>
5. Shi Y Guang, (2016) Research on seismic properties and thermal performance of cotton straw brick houses. *Xinjiang Agricultural University*, 3-5. https://hfffgc1d129f57bb244a4snu9cknf6nk006o0ufgfy.eds.tju.edu.cn/kcms2/article/abstract?v=3uoqIhG8C475K0m_zrgu4IQARvep2SAkkyu7xrzFWukWlylpgWWcEl8r_Xn0m7VQIyrSF0Hd7BSxIPU3F19npsGmZPwfCAu&uniplatform=NZKPT
6. Minke G, Mahlke F, (2005) *Building with Straw*. https://discovered.ed.ac.uk/permalink/44UOE_INST/iatqhp/alma9912671113502466

7. Drack M, Wimmer R, Hohensinner H. (2004) Treeplast screw – a device for mounting various items to straw bale constructions. *The Journal of Sustainable Product Design*, **4** 33-41. <https://doi.org/10.1007/s10970-006-0001-z>
8. Ministry of Housing and Urban-Rural Development of the People's Republic of China, (2015) *Technical Specification for In-situ Measurement of Thermal Transmittance of Building Envelope*. China Architecture & Building Press, 7-8. <https://www.mayiwenku.com/p-24966005.html>
9. Wang J, Xu L, Long E Sheng, (2014) Experimental Research on Thermal Performance of Lightweight Envelope Integrated with Phase Change Material, *Proceedings of the 8th International Symposium on Heating, Ventilation and Air Conditioning*, (Indoor and Outdoor Environment vol 1) ed Li A Gui, Zhu Y Xin and Li Y Guo, (Springer: Springer Heidelberg New York Dordrecht London) pp275-280. <https://doi.org/10.1007/978-3-642-39584-0>
10. Ministry of Housing and Urban-Rural Development of the People's Republic of China. (2012) *Design Code for Heating, Ventilation and Air Conditioning in Civil Buildings*. China Architecture & Building Press, 12-13. <http://www.jianbiaoku.com/webarbs/book/16582/1663584.shtml>
11. Gao Y, Hu K, Ding C, Yao S, Yuan J Yu, (2021) Multi-objective optimization for low-carbon retrofit of “Double Substitution” rural houses in Hebei plain. *Science Technology and Engineering*, **21** 8565-8573. https://hfffgcl1d129f57bb244a4snu9cknf6nk006o0ufgfy.eds.tju.edu.cn/kcms2/article/abstract?v=3uoqIhG8C44YLTlOAIrTKibYIV5Vjs7iy_Rpms2pqwbFRRUtoUImHZK3Encwfg6NzOAcT5U6wVKZviQN2eCdcgdPzX7wsjCP&uniplatform=NZKPT

Open Access This chapter is licensed under the terms of the Creative Commons Attribution-NonCommercial 4.0 International License (<http://creativecommons.org/licenses/by-nc/4.0/>), which permits any noncommercial use, sharing, adaptation, distribution and reproduction in any medium or format, as long as you give appropriate credit to the original author(s) and the source, provide a link to the Creative Commons license and indicate if changes were made.

The images or other third party material in this chapter are included in the chapter's Creative Commons license, unless indicated otherwise in a credit line to the material. If material is not included in the chapter's Creative Commons license and your intended use is not permitted by statutory regulation or exceeds the permitted use, you will need to obtain permission directly from the copyright holder.

